Supplementary information for:

Insights into the polymorphism of $Bi_2W_2O_9$: single crystal growth and a complete survey of the variable-temperature thermal and electrical properties

Xiangxin Tian, Zeliang Gao,* Feifei Chen, Qian Wu, Conggang Li, Weiqun Lu, Youxuan Sun, and Xutang Tao*

State Key Laboratory of Crystal Materials, Shandong University, Jinan, Shandong 250100, China

Table S1 Atomic coordinates and equivalent isotropic displacement parameters for $Bi_2W_2O_9$.

	x	y	z	U_{eq}
Bi(1)	0.3041(1)	0.2303(1)	0.8540(a)	0.08(1)
W(1)	0.4232(1)	0.2557(1)	1.3354(1)	0.04(1)
O(1)	0.3477(3)	0.1869(12)	1.2779(13)	0.09(1)
O(2)	0.2501(2)	-0.0100(10)	1.0781(11)	0.07(1)
O(3)	0.4333(3)	-0.0469(12)	1.0780(12)	0.10(1)
O(4)	0.4120(3)	0.4640(11)	1.0021(14)	0.09(1)
O(5)	0.5000	0.3075(16)	1.2500	0.08(2)

U_{eq} is defined as one third of the trace of the orthogonalized U_{ij} tensor.

Table S2 Selected bond lengths (Å) and angles (º) for $Bi_2W_2O_9$ crystal structure

Selected bond lengths (Å)			
Bi(1)-O(2)	2.194(5)	W(1)-O(3)#4	1.753(7)
Bi(1)-O(2)#1	2.260(5)	W(1)-O(4)#5	1.788(6)
Bi(1)-O(2)#2	2.304(5)	W(1)-O(1)	1.855(7)
Bi(1)-O(2)#3	2.488(5)	W(1)-O(5)	1.899(1)
Bi(1)-O(1)#2	2.519(7)	W(1)-O(4)	2.150(7)
Bi(1)-O(1)	2.536(7)	W(1)-O(3)	2.168(7)
Selected bond angles (º)			
O(2)-Bi(1)-O(2)#3	113.23(11)	O(1)-W(1)-O(5)	156.0(2)
O(2)#1-Bi(1)-O(1)#2	151.6(2)	O(3)#4-W(1)-O(4)	171.3(3)
O(2)#2-Bi(1)-O(1)	140.3(2)	O(4)#5-W(1)-O(3)	170.2(3)

Symmetry transformations used to generate equivalent atoms: #1 -x+1/2,y+1/2,z; #2 x,-y,z-1/2; #3 -x+1/2,-y+1/2,z-1/2; #4 x,-y,z+1/2; #5 x,-y+1,z+1/2; #6 -x+1/2,y-1/2,z

Table S3 Direction and magnitude of the WO_6 octahedron and BiO_8 polyhedron in $Bi_2W_2O_9$

asymmetric units	octahedron distortion, Δd		dipole moment				
	direction	magnitude	x (a)	y (b)	z (c)	magnitude	
						debye	$\times 10^{-4}$ esu.cm/Å^3
WO_6	C_2 [110]	0.835	1.0730	-0.5640	-1.6608	2.0561	117.9
BiO_8	-	-	4.8569	11.7750	3.7350	13.2737	761.1

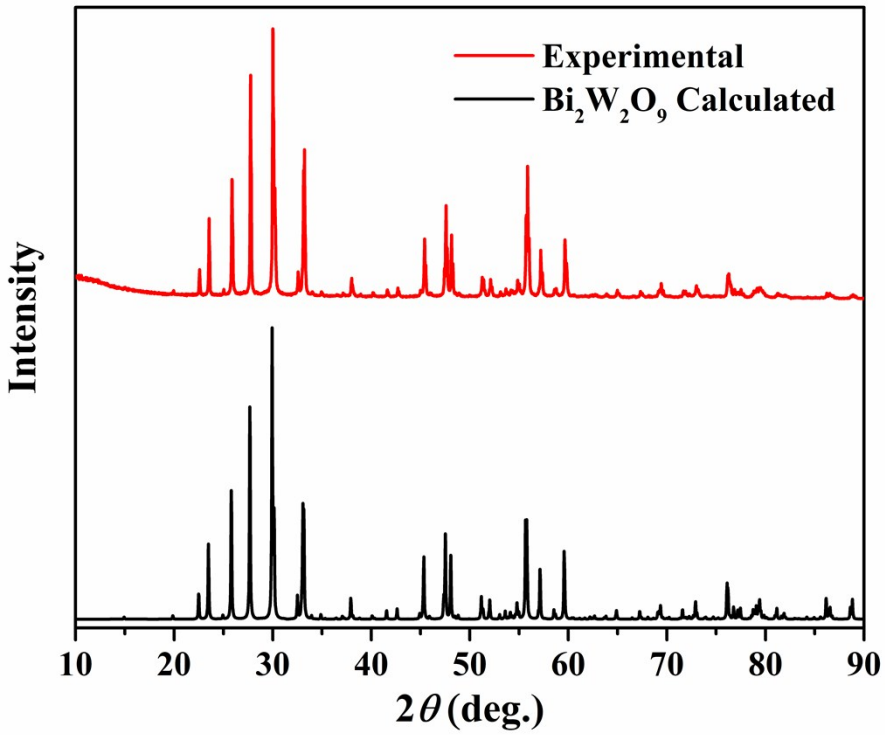

Fig. S1 Comparison of the experimental and calculated powder X-ray diffraction patterns for polycrystalline $Bi_2W_2O_9$ sintered at 750 ºC.

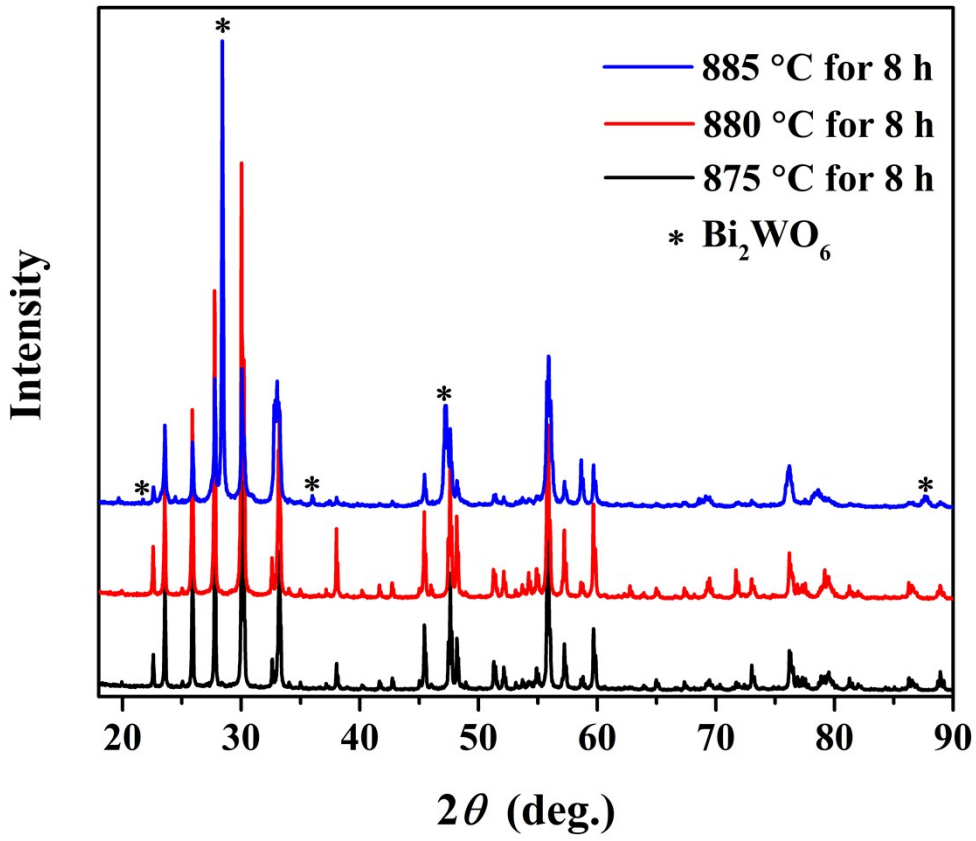

Fig. S2 Room temperature X-ray diffraction patterns for $Bi_2W_2O_9$ ceramics sintered at 875, 880, and 885 ºC, respectively, for 8 h.

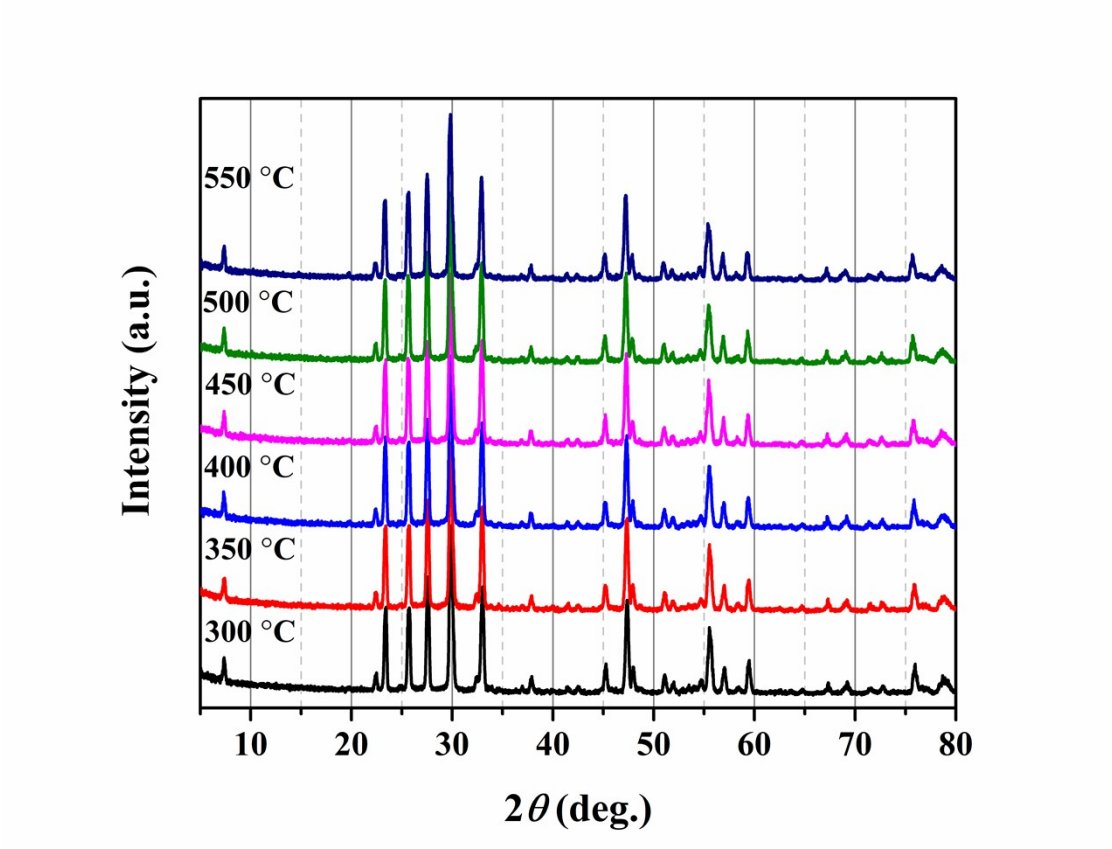

Fig. S3 (a) In situ PXRD patterns for $Bi_2W_2O_9$ powders in the temperature range 300-550 ºC.

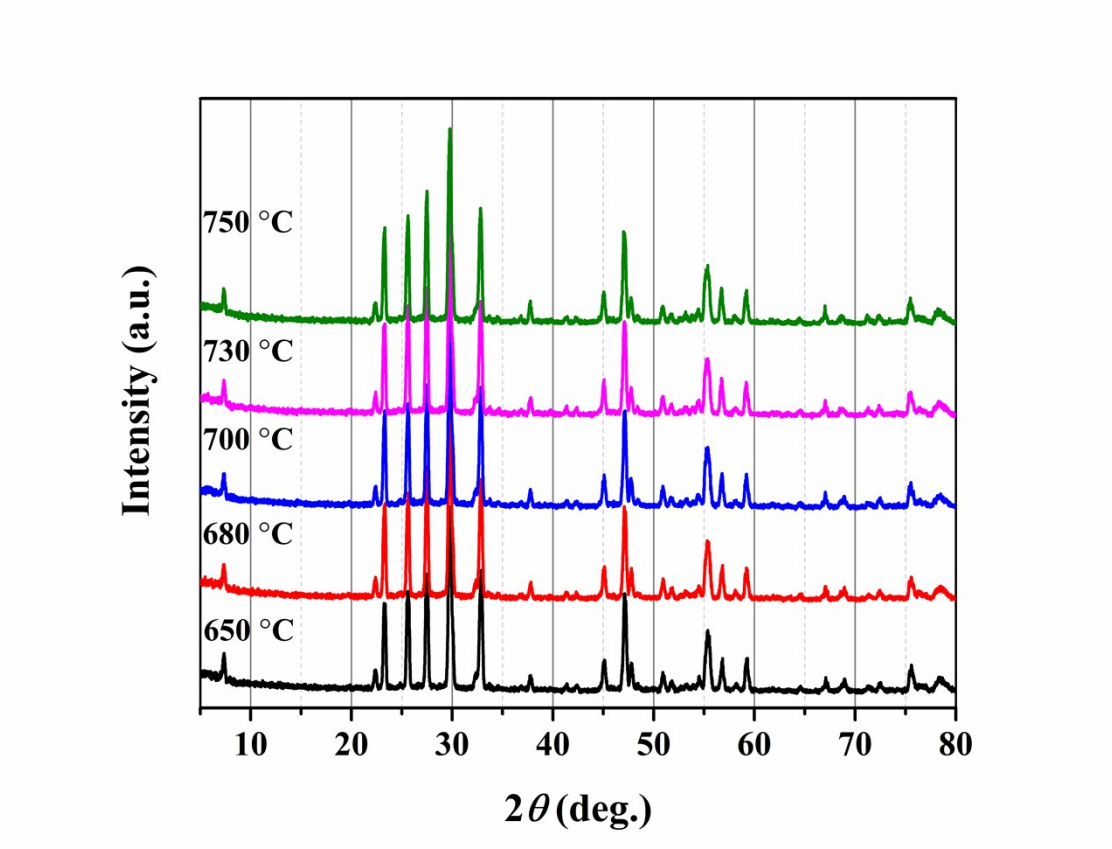

Fig. S3 (b) In situ PXRD patterns for $Bi_2W_2O_9$ powders in the temperature range 650-750 ºC.

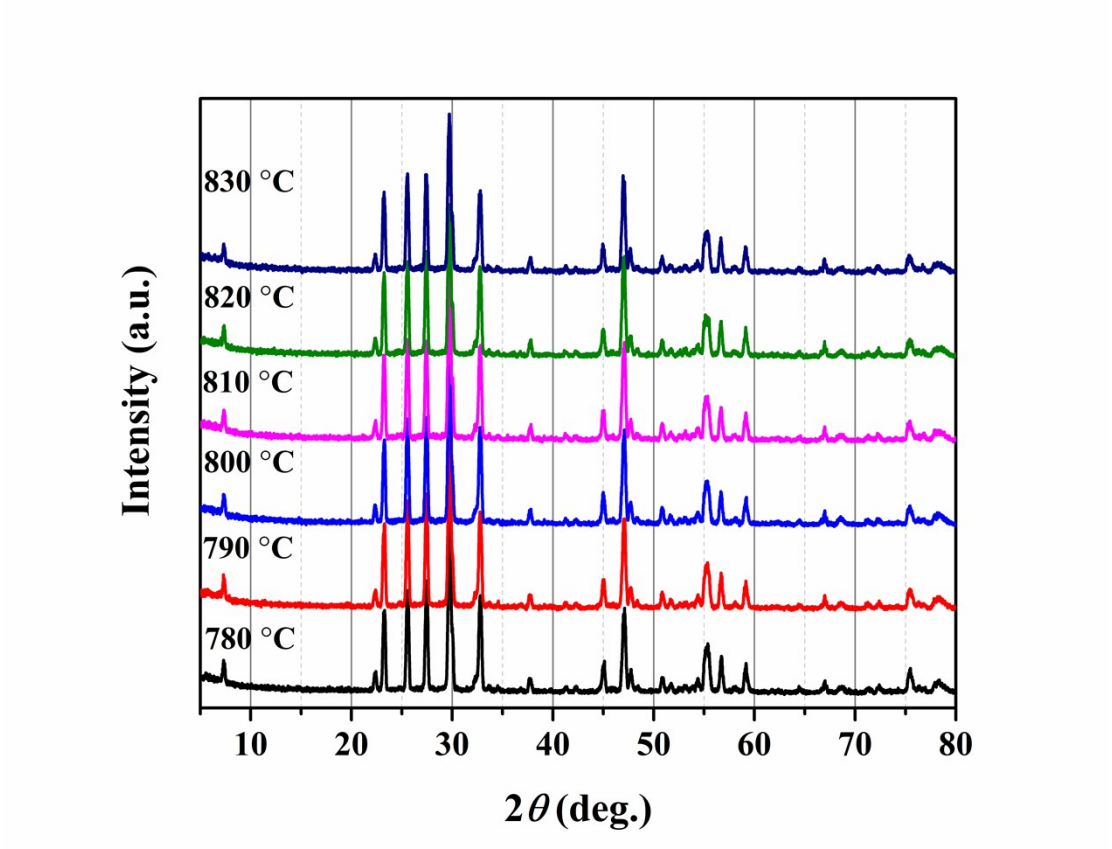

Fig. S3 (c) In situ PXRD patterns for $Bi_2W_2O_9$ powders in the temperature range 780-830 ºC.

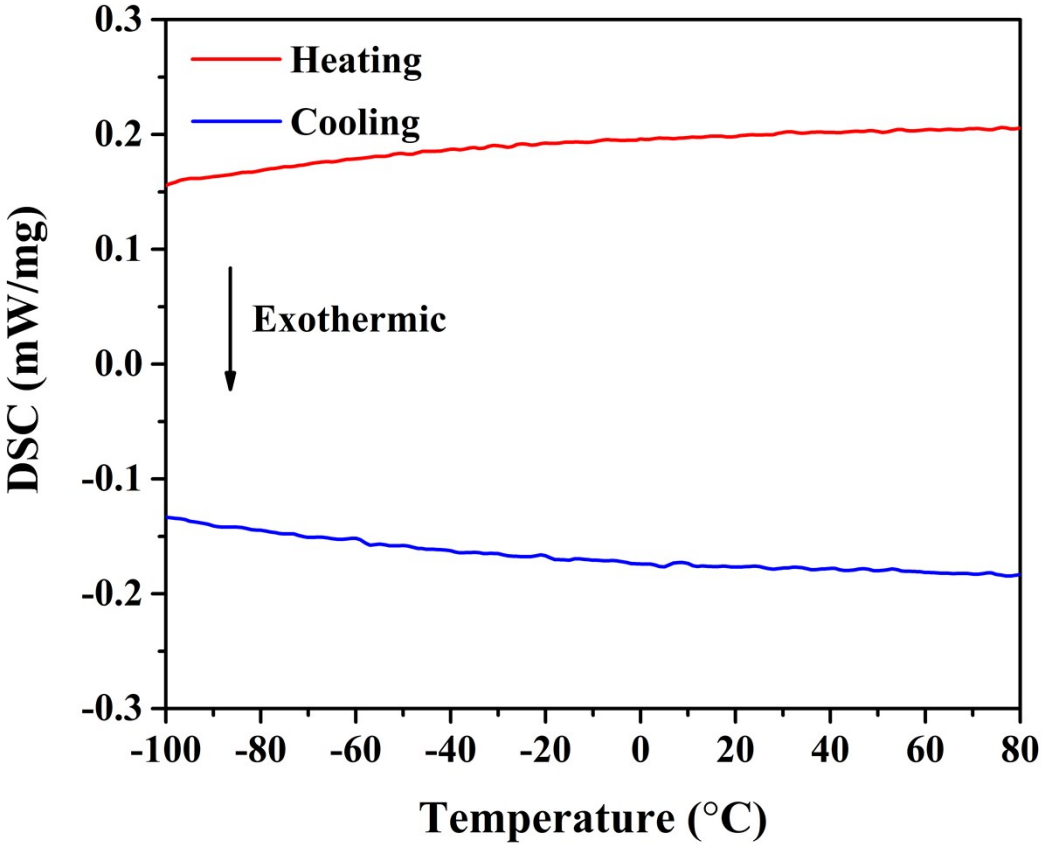

Fig. S4 Low temperature DSC data for $Bi_2W_2O_9$ in the range of -100 to 80 ºC at a heating/cooling rate of 10 ºC/min.

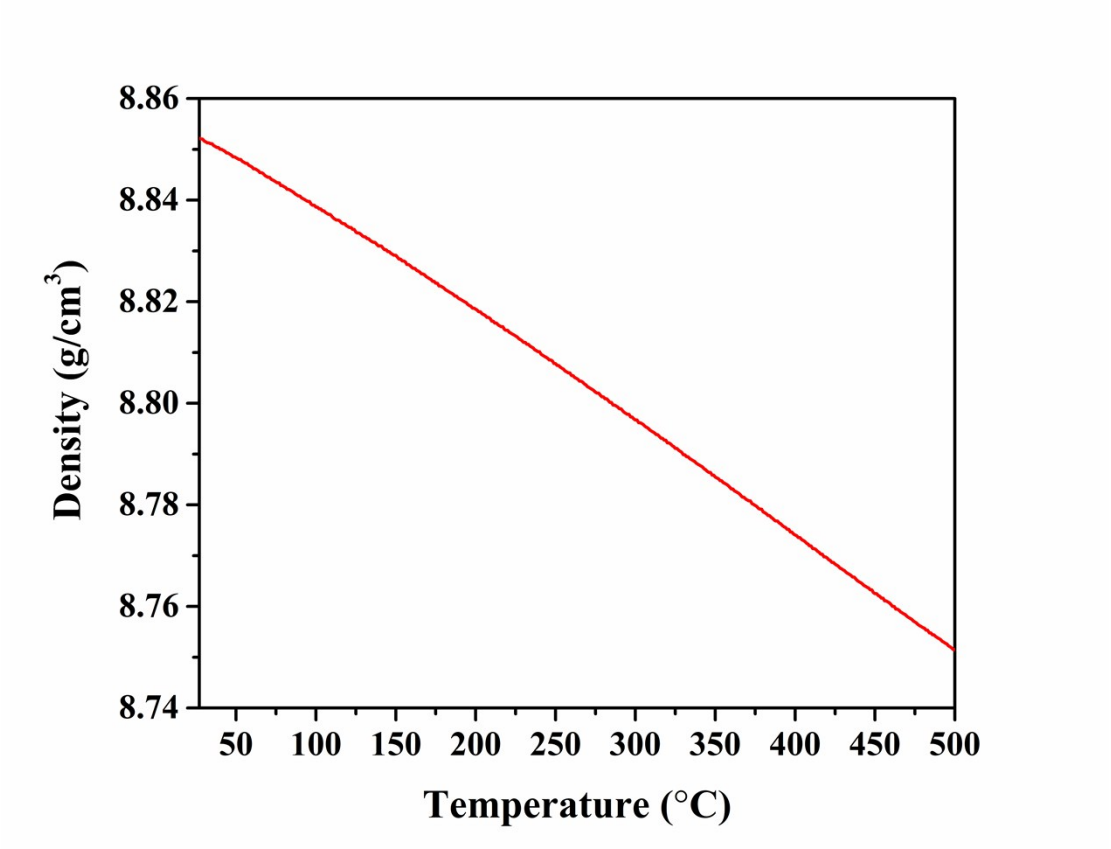

Fig. S5 Calculated density vs. temperature of $Bi_2W_2O_9$.